Applied Catalysis B: Environmental 100 (2010) 271–281

Contents lists available at ScienceDirect

Applied Catalysis B: Environmental

journal homepage: www.elsevier.com/locate/apcatb

Effect of the atomic active metal ratio in Al/Fe-, Al/Cu- and Al/(Fe–Cu)-intercalating solutions on the physicochemical properties and catalytic activity of pillared clays in the CWPO of methyl orange

Luis Alejandro Galeano[a,*], Antonio Gil[b], Miguel Angel Vicente[c]

[a] Grupo de Investigación en Materiales Funcionales y Catálisis GIMFC, Departamento de Química, Universidad de Nariño, Calle 18, Cra. 50 Campus Torobajo, Pasto, Colombia
[b] Departamento de Química Aplicada, Universidad Pública de Navarra. Edificio Los Acebos, Campus de Arrosadía, Pamplona 31006, Spain
[c] Departamento de Química Inorgánica, Facultad de Ciencias Químicas, Universidad de Salamanca. Plaza de la Merced, s/n, Salamanca 37008, Spain

ARTICLE INFO

Article history:
Received 20 April 2010
Received in revised form 30 July 2010
Accepted 5 August 2010
Available online 12 August 2010

Keywords:
Pillared clays
Azo dye methyl orange
Catalytic wet peroxide oxidation

ABSTRACT

The effect of the composition of the intercalating solutions in the catalytic performance of the derived pillared clays has been studied. A Colombian bentonite was treated with Al/Fe-, Al/Cu- and Al/(Fe–Cu)-solutions, and the resulting pillared solids were used in the catalytic wet peroxide oxidation (CWPO) of the azo dye methyl orange (MO) in aqueous solutions. The active metal ratio (AMR), here defined as the atomic percent ratio between the active metals (Fe and Cu) and the total content of metals (Al, Fe and/or Cu) in the intercalating solutions, was found to be a key factor for the properties of the pillared solids. Low AMR values, between 0 and 10%, were considered, and the efficiency for the incorporation of the active metals into the layered structure was followed by chemical analyses and cationic-exchange capacity measurements. Further characterization studies were carried out by X-ray diffraction, H_2 temperature-programmed reduction, scanning electron microscopy/energy dispersive X-ray analysis, nitrogen adsorption at −196 °C and thermal analysis. Considering the physicochemical properties together with the catalytic performance, it is proposed that isomorphic incorporation of the active metals into the Al_{13}-like polycations may take place. The obtained pillared solids exhibited better catalytic performance as the AMR values were lowered in the corresponding intercalating solutions, displaying also high stability to chemical leaching into the strongly oxidizing environment of the catalytic reaction, especially in the binary Al/Fe- and Al/Cu-systems. The Al/Fe-pillared clays attained most of their maximal removal of the azo dye in solution after only 1 h of reaction at very mild experimental conditions (room temperature and atmospheric pressure of 18 °C and 0.7 atm).

1. Introduction

The catalytic abatement of toxic organic compounds in wastewaters has been extensively studied in the last years; from this kind of compounds, phenols and azo dyes have received much attention [1–7]. The last group comes mainly from the textile industry, providing toxic and highly coloured water streams wherein the penetration of solar radiation is significantly restricted, decreasing seriously the photosynthetic activity of biological agents in the aquatic environments affected [8]. Advanced oxidation processes (AOPs) have been widely proposed for elimination of these hazardous compounds, particularly when they are in low concentrated effluents. AOPs are a set of catalytic, photocatalytic, photolytic, etc. technologies, addressed towards a continuous generation of hydroxyl radicals (HO•), which are able to deplete a wide range of organic substances otherwise difficult to biodegrade [9–12]. Thus, although the well known Fenton-like activated peroxide elimination of organic compounds, carried out by cations of metals like Fe or Cu in homogeneous phase would fulfil the general requirements for AOPs, strong efforts have lately been made in order to develop solid catalysts able to perform the same activation of peroxide under heterogeneous conditions, then avoiding the expensive and difficult recovery of the metal from the effluent at the end of the treatment. AOP operated with this kind of active solids under very mild conditions of atmospheric pressure and room temperature has been referred to by some authors as Catalytic Wet Peroxide Oxidation (CWPO) [13–16]. Several solid materials have been claimed as being active to catalyse the Fenton-like reaction, among them: iron-containing zeolites, polymer-supported metal complexes, carbon-supported metal oxides, iron mesoporous materials, etc. [10,17–21]. However, the high performance displayed by Fe,Cu-modified pillared clays (Fe,Cu-PILCs) in this reaction is remarkable, achieving high rates of elimination of several model toxic compounds in terms of both, simple contaminant depletion as well as

* Corresponding author. Tel.: +57 2 7313106; fax: +34 923 294574.
E-mail address: alejandrogaleano@udenar.edu.co (L.A. Galeano).

0926-3373/$ – see front matter © 2010 Elsevier B.V. All rights reserved.
doi:10.1016/j.apcatb.2010.08.003

total organic carbon (TOC)/chemical oxygen demand (COD) elimination. Moreover, these catalysts can be obtained from inexpensive raw materials by means of very simple water-based chemical operations [1–4,14,22,23].

Several studies have pointed out that smectites pillared with Al-based polycations containing iron or copper are materials that show high performance catalysing the CWPO reaction [3,13,14,23–25]. Recently, Timofeeva et al. have reported the effect of some synthesis variables, like hydrolysis ratio of the pillaring solution (OH/(Al + Fe)) and temperature of calcination in the preparation of Fe/Al-PILCs [3], as well as the effect of the atomic ratio Fe/Cu in Fe,Cu,Al-clays on the catalytic properties of the resulting materials in the CWPO reaction [4]. It is worth noting here that the presence of Cu or Fe isolated species in this kind of materials should be ascribed to their intercalation by means of truly mixed Al/M-polycations. Although, despite the variety of experimental techniques displayed in many previous works [2,3,14,22,26–34], it is not absolutely and widely accepted that iron or copper could substitute aluminium in the Keggin-like polycation network. Although a close correlation between catalytic activity and concentration of isolated Fe species has been repeatedly claimed in these systems, not enough work has been carried out in order to establish the optimum conditions of preparation under which the catalytic response of Al/Fe-, Al/Cu- and Al/(Fe–Cu)-pillared clays in the CWPO reaction is improved in terms of catalytic activity and chemical stability of the active metals to leaching.

Therefore, this work is devoted to establish if a relationship takes place between the atomic metal ratio of the active metals (Fe and/or Cu), as an important synthesis variable in Al-based mixed intercalating solutions, and the physicochemical properties and catalytic behaviour of the obtained pillared clays in the CWPO elimination of the hazardous organic, azo dye methyl orange in aqueous solutions. Besides, the study will allow a correlation between the key properties of the materials, allowing proposing about the nature of the true metal species of Fe and Cu that are stabilized by mixed pillaring of smectites with Al and their possible catalytic role in the CWPO reaction.

2. Experimental

2.1. Materials

The starting material was a natural bentonite mined by Bentocol S.A. from the Valle del Cauca region, Colombia. The mineral was used in two commercial forms:

(i) The solid received as mined and then particle size refined at lab scale by separation of the $\leq 2\,\mu m$ fraction (denoted BV). This fraction was mainly composed of montmorillonite; it had the chemical composition 60.5% SiO_2, 24.7% Al_2O_3, 10.2% Fe_2O_3, 0.05% MnO, 3.07% MgO, 0.64% CaO, 0.20% Na_2O, 0.58% K_2O; and its Cation Exchange Capacity (CEC), was 89 mequiv./100 g.
(ii) The mined solid submitted to homoionization with sodium as preferential compensating cation (process carried out by Bentocol at its own industrial plant), and followed by lab extraction of the $\leq 2\,\mu m$ fraction (denoted NaBV). Its CEC was 87 mequiv./100 g.

For the experiments of intercalation and pillaring, $AlCl_3{\cdot}6H_2O$ (99%), $Fe(NO_3)_3{\cdot}9H_2O$ (99.99%) and $CuCl_2{\cdot}2H_2O$ (99.999%), all from Sigma–Aldrich, were employed as received. For the catalytic runs, methyl orange (MO), ACS reagent (>85%) from Sigma–Aldrich ($C_{14}H_{14}N_3NaO_3S$) and hydrogen peroxide (30%, w/w, A.R. from Panreac) were also used as received.

2.2. Preparation of pillared clays

The preparation of the pillared clays was carried out following a conventional procedure described in detail by Barrault et al. [13]. The corresponding starting clay was stirred (2 wt.% suspension) in distilled water for 24 h at room temperature. In each series, the starting clays were pillared with single Al hydrolysed solution (samples NaAl and BVAl, respectively). For the mixed systems, the Al/Fe-, Al/Cu- or Al/(Fe–Cu)-intercalating solutions were prepared by mixing various volumes of 0.2 M $AlCl_3{\cdot}6H_2O$, 0.02 M $Fe(NO_3)_3{\cdot}9H_2O$ and/or 0.02 M $CuCl_2{\cdot}2H_2O$, to reach AMR values below 10%. When both Fe and Cu were added together into the intercalating solutions, their mole ratio was always kept constant in 1.0. Thereafter, a 0.2 M NaOH solution was slowly added at 70 °C in enough amount to get hydrolysis ratio (OH/(Al + M)) of 2.0 (M = Fe, Cu or (Fe + Cu)). The resulting solution was then aged at the same temperature for 2 h, left to reach room temperature and slowly dropped (1.5 mL/min) to the clay suspension, under strong shaking. The resulting mixture was stored 24 h at the same temperature. The intercalated clay was filtered by suction, repeatedly washed with distilled water, dried at 60 °C and calcined at 500 °C for 2 h. The designation of the samples denotes the form of the clay employed as starting material (BV or NaBV), the pillaring metals (Al, Fe and/or Cu), finishing with the AMR value (see Table 1).

The AMR value is defined as the atomic percent ratio between the active metals (Fe and/or Cu) and the total content of metals (Al, Fe and/or Cu). For instance, AMR values for the system Al/Fe can be calculated as follows:

$$\text{AMR}\ \ (\%) = \left(\frac{\text{mmol Fe}}{\text{mmol Fe} + \text{mmol Al}}\right) \times 100$$

where "mmol" of every metal corresponds with the true amount of that metal present in the final intercalating solution added on the clay suspension.

2.3. Physicochemical characterization

Elemental chemical analyses of the solids were carried out by Activation Laboratories Ltd., Ancaster – Ontario, Canada, using inductively coupled plasma spectroscopy (ICPS). The monitoring for concentration of Fe and/or Cu leached in the effluent after the catalytic tests was made by atomic absorption spectroscopy (AAS) in a Perkin Elmer 2380 spectrometer.

The cationic-exchange capacity (CEC) of the materials was determined by saturation with 1 M ammonium acetate solution under reflux, followed by repeated washing with distilled water and centrifugation to eliminate excess of ammonium ions. The retained ammonium ions were then determined by the micro-Kjeldahl method.

X-ray diffraction (XRD) patterns of the solids were recorded over powder solids or oriented films by using a Siemens D-500 diffractometer, working at 40 kV and 30 mA with a scanning speed of 2°/min, employing Cu Kα filtered radiation (λ = 1.5418 Å).

Textural properties were determined from nitrogen (Air Liquide, 99.999%) adsorption data, obtained at −196 °C with a Micromeritics Gemini 2375 apparatus. Specific surface areas were obtained from the BET method; external surface areas and micropore volumes by means of the *t*-method, and the total pore volume from the nitrogen adsorbed at a relative pressure of 0.95.

Thermal analyses were performed on a SDT Q600 TA analyser, for simultaneous gravimetric and DSC analyses. All measurements were carried out at a heating rate of 10 °C/min under a flow of 20 mL/min of oxygen (Air Liquide, 99.999%) up to 1000 °C.

Hydrogen temperature-programmed reduction analyses (H_2-TPR) were carried out in a Micromeritics TPR/TPD 2900 instrument. Around 40 mg of sample were heated from room temperature to

Table 1
Al, Fe and Cu content of pillaring solutions and solid materials, and CEC compensation (CC).

Sample	AMR (%)	Pillaring sln. content	Solid content (wt.%)[a]			Fe_{added} (Fe_2O_3 wt.%)	CC (%)[b]
		Al/Fe/Cu (mol/mol/mol)	Al_2O_3	Fe_2O_3	CuO		
NaBV	NA	NA	26.4	6.95	0.00	NA	NA
NaAl	0	100/0/0	32.5	7.49	0.00	NA	62
NaAlFe2	2	98/2/0	36.0	8.37	0.00	1.42	55
NaAlFe4	4	96/4/0	35.4	9.83	0.00	2.87	44
NaAlFe6	6	94/6/0	37.8	10.3	0.00	3.31	41
NaAlFe8	8	92/8/0	39.0	11.1	0.00	4.14	34
NaAlFe10	10	90/10/0	38.2	11.4	0.00	4.48	26
NaAlCu2	2	98/0/2	38.4	8.31	0.12	NA	54
NaAlCu4	4	96/0/4	39.2	7.97	0.14	NA	50
NaAlCu6	6	94/0/6	47.5	9.85	0.24	NA	56
NaAlCu8	8	92/0/8	41.5	7.86	0.22	NA	37
NaAlCu10	10	90/0/10	45.8	8.66	0.26	NA	47
NaAlFeCu2	2	98/1/1	35.0	7.68	0.12	NA	46
NaAlFeCu4	4	96/2/2	28.3	7.76	0.03	NA	44
NaAlFeCu6	6	94/3/3	37.5	8.38	0.11	NA	41
NaAlFeCu8	8	92/4/4	37.7	8.73	0.18	NA	65
NaAlFeCu10	10	90/5/5	37.0	9.33	0.03	NA	68
BV	NA	NA	24.7	10.2	0.00	NA	NA
BVAl	0	100/0/0	33.6	10.1	0.00	NA	81
BVAlFe1	1	99/1/0	33.6	10.6	0.00	0.65	76
BVAlFe2	2	98/2/0	34.1	11.2	0.00	1.29	55
BVAlFe5	5	95/5/0	33.9	13.1	0.00	3.14	45
BVAlCu1	1	99/1/0	35.2	10.0	0.06	NA	63
BVAlCu3	3	97/3/0	38.0	10.0	0.22	NA	55
BVAlCu5	5	95/5/0	40.8	10.1	0.51	NA	53
BVAlFeCu3	3	97/1.5/1.5	35.0	10.9	0.09	0.94	47
BVAlFeCu5	5	95/2.5/2.5	36.1	11.5	0.17	1.58	47

NA = not applicable for this sample.
[a] Contents referred to the SiO_2 content in the starting clay for each series (68.7% for NaBV; 60.5% for BV) (dry-basis).
[b] CC (%) = percentage of the cationic-exchange capacity of the starting material that was compensated by the intercalating solution.

900 °C at 10 °C/min, under a total flow of 60 mL/min of carrier gas (5% H_2 in air, Air Liquide). Hydrogen consumption was measured by a thermal conductivity detector (TCD) and CuO (Merck, 99.99%) was used as external standard for area calibration.

Scanning electron microscopy (SEM) of the materials was performed in a Digital Scanning Microscope DSM940 Zeiss operated at 15 kV, in *Servicio General de Microscopía Electrónica*, University of Salamanca. The samples were coated with a thin gold layer by evaporation using a Bio-Rad ES 100 SEN coating system in order to enhance the electric conductivity of the surface.

2.4. Catalytic tests

Chemical oxidation of the azo dye methyl orange was carried out using 100 mL of a 100 mg/L solution (typical waste streams from the textile industry exhibit concentrations slightly below this value [1,35]), in a glass semi-batch reactor of 250 mL operating at room temperature and atmospheric pressure (18 °C, 0.7 atm), with continuous stirring of the reaction mixture by a magnetic stirrer (200 rpm). The pH of the reaction mixture was continuously monitored with a pH-meter from Denver Instruments. In order to keep it constant at the desired value, solutions 1 M of H_2SO_4 or NaOH were dropped when needed. The optimum pH values for each metallic system were adjusted according with literature in 3.7 for Al/Fe-PILCs and 5.5 for Al/Cu-PILCs [13,14,36,37]. The optimum value for Al/(Fe–Cu)-PILCs was arbitrary set in 4.6, the average of the values reported for the binary systems. 0.5 g of catalyst were added into the reaction vessel and the mixture kept under stirring by additional 15 min. Air bubbling at a constant flow rate was maintained throughout all the experiment and once the pH of the reaction mixture was adjusted to the corresponding set value, 8.0 mL of fresh-prepared 0.15 M hydrogen peroxide started to be fed into the system under a flow rate of 2.0 mL/h (The H_2O_2 added is 0.9 times the stoichiometric amount for complete oxidation of MO, according to the equation: $C_{14}H_{14}N_3O_3SNa + 43H_2O_2 \rightarrow 14CO_2 + 3HNO_3 + NaHSO_4 + 48H_2O$.) A Fisher Scientific peristaltic bomb was used for this purpose. The beginning of the H_2O_2 addition was taken as zero time point of the reaction, and the periodic sampling was made throughout 4 h of reaction in all the experiments.

Samples of 2.0 mL were micro-filtered (Millipore, cellulose acetate, 0.45 μm) immediately after taken from the reactor at various times and analysed to determine the MO concentration. The measurements of absorbance were recorded at 486 nm (HACH 2010 spectrophotometer), the experimental wavelength found for the maximum absorption in visible range of the azo dye MO at pH 3.7, as no significant differences were observed in sensibility nor linearity when monitoring the absorbance at slightly shifted analytical maximum wavelengths found for the other catalytic systems (Al/Cu: pH 5.5, λ_{max} = 465 nm; Al/(Fe–Cu): pH 4.6, λ_{max} = 473 nm). The reaction mixtures were left to settle for further 24 h after the last sampling, and then filtered by suction, the resulting solution being submitted to chemical analyses to find leached iron and copper. Although a fraction of the leached iron might undergo subsequent partial precipitation as Fe(III) hydroxide, this method enabled to test the stability of the catalysts for a longer period of time into the reaction mixture.

3. Results

3.1. Effect of AMR value on the insertion of the active metals

The elemental composition of pillaring solutions and pillared solids are shown together with AMR values and abbreviated designation of samples in Table 1. In order to better compare the changes induced by the treatments in the chemical composition of the solids, their contents of Al_2O_3, Fe_2O_3 and CuO were normalized to the content of SiO_2 in the corresponding starting mineral

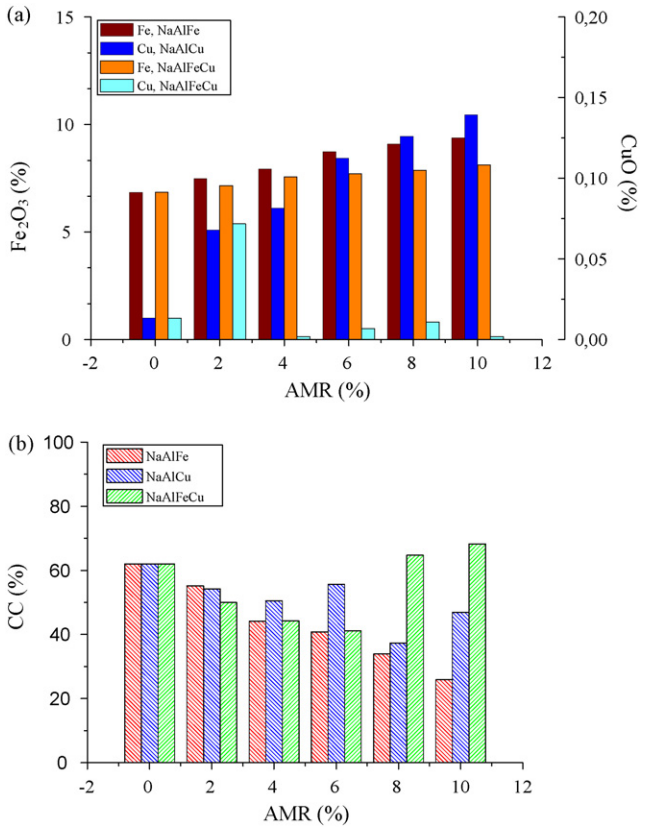

Fig. 1. Active metal content and compensation of cationic charge in NaBV-PILCs, at increasing AMR values: (a) Fe_2O_3 and/or CuO SiO_2-normalized mass percentage; (b) compensation of cationic charge (CC %) for each catalytic system.

(68.7% for NaBV-series; 60.5% for BV-series), assuming that SiO_2 content is not affected by the treatments carried out, that is, this element remains in the solids during all the preparative process. First of all, it is noteworthy that Al^{3+} is the more abundant cation in the octahedral layer; the raw clay being strongly dioctahedral. The relative high content of Fe_2O_3 also suggests a not negligible presence of this element in the clay layers [38]. Besides, the SiO_2 content is clearly higher in the NaBV-derived solids than in the BV-derived ones, which can be attributed to the presence of quartz as impurity in the Na-commercial form of the clay, which was not completely removed during the particle size separation step, probably due to the addition of a tensioactive by the manufacturer in order to enhance the rheological properties of the clay. Such addition avoids the correct separation of the clay fractions by decantation.

As already said, the Fe content in the starting materials was rather high, and this content only decreases around one third from BV to NaBV, in spite of the long treatment applied to NaBV. This suggests that most of this element is in the clay as octahedral cation, while a small amount can be present as extra-framework oxide aggregates. Furthermore, previous studies carried out on the same raw mineral showed that its iron content only decreased very slightly even after thorough purification treatment (elimination of soluble salts, carbonates, organic matter and finally free iron oxides by leaching with sodium citrate/sodium dithionite) [23]. As expected, the Cu content in the starting clays is negligible.

The mass percentage of each active metal in the pillared solids as a function of the AMR values in the intercalating solutions is shown in Fig. 1a. It can be seen that for the binary systems Al/Fe- and Al/Cu-PILCs the contents of both, iron and copper, rise in a uniform trend, although faster for the last one. However, it is also very important to note that the contents of Cu stabilized are very low,

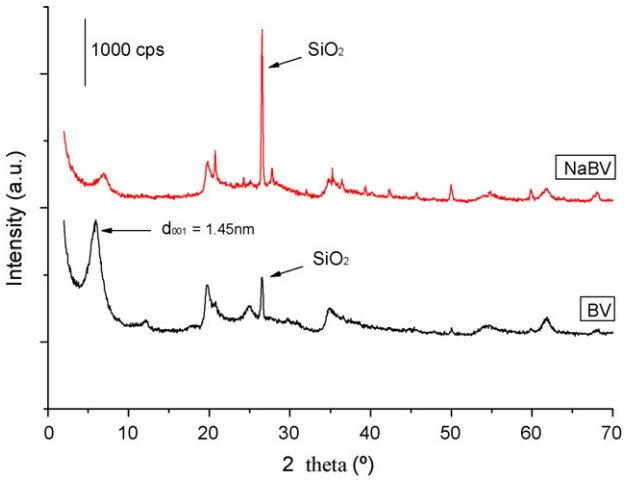

Fig. 2. Powder X-ray diffraction patterns of starting materials. Na-form of the starting refined smectite NaBV (up). Natural starting refined smectite BV (down).

being incorporated in amounts in average ca. 15 times lower than Fe for equivalent AMR values. This value is verified in terms of the atomic ratio $Fe_{stabilized}/Cu_{stabilized}$ (14.90), which is obtained by simple comparison of the contents of such metals in SiO_2-normalized compositions, discounting in advance the amount of iron present in the parent solid NaAl. The low ability of Cu to be stabilized in Al/Cu-PILCs by conventional pillaring procedures has been well documented [36,39], as long as new preparative strategies have also been recently explored in order to overcome such a drawback [40]. This is probably related to a lower ability of Cu^{2+} to isomorphically substitute Al^{3+} in the Keggin polycation, as it is discussed in more detail in a forthcoming section.

The efficiency for the cationic charge compensation (CC) was higher than 40% in all the pillared solids (Fig. 1b), when CC is defined as the fraction of the initial CEC that was successfully compensated with no longer exchangeable (oligo)cations, stabilized during the steps of the pillaring procedure (intercalation and subsequent calcination). For the Al/Fe-PILCs series, there is a lower efficiency to compensate the interlayer charge as the AMR value in the pillaring solution increases. Such charge compensation is expected to be carried out mainly by condensed polycations; however, this behaviour is not observed for any of the other two mixed metallic systems studied (Al/Cu and Al/Fe–Cu).

When the amount of iron in the intercalated solution increases, the formation of low-condensed polymeric species with the subsequent decrease in the amount of tridecameric Keggin-like polycations may take place, because the more acidic nature of Fe^{3+} with respect to Al^{3+} leads to a slightly lower final pH after the ageing process (it may be considered that the ratio OH/metal was the same for all the polymerizations). These small variations in the pH of the intercalating solutions may affect the speciation of aluminium in each system, which strongly depends on this variable [41,42] as well as the subsequent incorporation of Fe^{3+} and/or Cu^{2+} depends on the nature of the polymeric species formed. In the case of the Al/Cu system, the CC seems to be not affected by the AMR, varying randomly when increasing the fraction of Cu in the intercalating solutions, possibly because the low net amounts of the metal stabilized in these samples. In the case of he Al/Fe–Cu system, CC undergoes a minimum close to AMR = 6, increasing for higher AMR, which may be related to the formation of different kind of species, for instance mixed three-metallic oxides deriving in a different pattern of compensation of the clay's CEC.

The powder X-ray diffraction patterns of the starting materials are shown in Fig. 2. First of all, the main characteristic signals associated to smectites are observed, with the basal reflection close

Table 2
Thermal analysis, basal spacings and textural properties for a set of BV-derived PILCs.

Sample	T_{M1} (°C)[a]	Δm_1 (%)[b]	T_{M2} (°C)[a]	Δm_2 (%)[b]	d_{001}[c] (nm)	S_{BET} (m^2/g)	S_{EXT} (m^2/g)	$V_{\mu p}$ (mL/g)	$V_{p\ total}$ (mL/g)
BV	114	8.38	491	3.23	1.45	93	61	0.016	0.100
BVAl	105	11.46	487	3.56	1.92	155	77	0.038	0.120
BVAlFe1	107	12.90	492	3.04	1.99	140	75	0.036	0.113
BVAlFe2	107	12.66	490	3.44	1.97	155	90	0.037	0.129
BVAlFe5	104	11.94	488	2.96	1.90	130	75	0.040	0.121
BVAlCu1	103	12.24	485	3.18	1.98	129	65	0.035	0.107
BVAlCu3	103	13.86	484	3.18	1.96	172	87	0.048	0.133
BVAlCu5	100	13.09	481	3,11	2.08	123	62	0.034	0.098
BVAlFeCu3	111	11.50	487	3.36	1.97	147	80	0.037	0.122
BVAlFeCu5	110	12.18	487	3.04	1.94	150	82	0.038	0.129

[a] Temperature of the thermal effect, determined from the minimum of their endothermic DSC peaks.
[b] Mass loss values of the processes indicated in the previous column.
[c] Obtained from oriented samples.

to 6.0° (2θ) and the 0 6 0 reflection at ca. 62° (2θ), which identifies the clay phase as dioctahedral [43]. The BV sample contained a lower amount of quartz as impurity (characteristic reflection at 26.6° (2θ)), being consequently richer in clay. This is due to the rheological properties of the commercial Na-form, whose tensioactive content makes strongly difficult the particle size refining by gravity. This also explains why less-intense peaks were obtained in the powder X-ray diffraction patterns (not shown) of the NaBV-derived materials.

XRD patterns from oriented films of the intercalated/pillared BV-series solids (calcined under the same conditions than powder samples), demonstrated that the addition of the active metals, for a low content of the second metal (AMR = 1.0%), led to higher basal spacings compared to BVAl (i.e., d_{001} = 1.99 nm for BVAlFe1, d_{001} = 1.98 nm for BVAlCu1), but followed by decreasing values up to BVAlFe5 (d_{001} = 1.90 nm) or increasing values up to BVAlCu5 (d_{001} = 2.08 nm) as AMR raised to 5.0% (see Table 2). This may be due to the opposite change of pH induced by the addition of Fe or Cu to the pillaring solutions in comparison to the single Al-solution (e.g. BVAl pH = 4.61; BVAlFe1 pH = 4.40; BVAlCu1 pH = 4.65), with the consequences on the polymerization degree already discussed. Furthermore, it suggests that for Al/M mixed pillaring systems, controlling of the pH of the intercalating solutions might be preferred instead of the well known hydrolysis ratio (HR = OH/Al + M), which is more practical but depends on the acid–base properties of the second metal involved. The opposite trend in the basal spacing of the Al/Fe- and Al/Cu-systems may also reinforce the feasibility of the isomorphic substitution of these metals into the structure of the Al-based polycations, assuming that Al_{13} was promoted as main polycationic species in all solutions. By means of an alternative approach adopted by Sanabria et al. [44], formerly explored by O'Neil Parker et al. [32], the solid sulphates of the mixed Al/Fe pillaring precursors were directly characterized showing that there is a decrease in the *a* cell parameter detectable by XRD, as a higher amount of iron is incorporated to Al/Fe-PILCs. This has been related to isomorphous incorporation of iron into the Keggin polycation; *a priori*, such incorporation is possible, due to the similar ionic radii of octahedral Fe^{3+} (0.67 Å) and octahedral Al^{3+} (0.68 Å) (it must be underlined here that some references give a different value for the ionic radii of octahedral Al^{3+} (0.54 Å), fact that anyway does not change the discussion). Analogously, considering the ionic radii of octahedral Cu^{2+} (0.73 Å) [45], it can be proposed that the incorporation of Cu^{2+} into Al_{13} polycations might be also possible, although fairly less probable than that of Fe^{3+}. It correlates very well with the efficiency of insertion for these active metals already discussed, and also enables us to propose that insertion of Fe and Cu is mediated by intercalation of mixed polycations, as some of the main species stabilized in Al/M-PILCs. Hence, the CEC analyses did not provide a clear tendency for the charge compensation with the increasing AMR in the case of the Al/Cu-modified NaBV-derived materials, probably because the very low amounts of Cu inserted in these solids were not able to produce a significant change on the positive

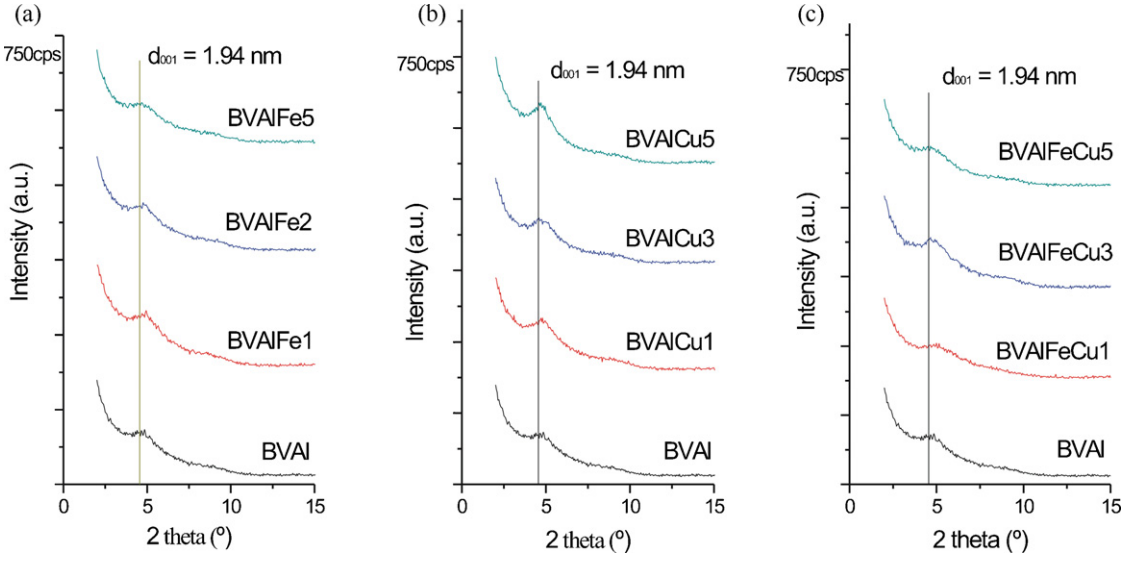

Fig. 3. Low angle region powder X-ray diffraction patterns for selected BV-modified materials. (a) Al/FeBV-PILCs; (b) Al/CuBV-PILCs; (c) Al/(Fe–Cu)BV-PILCs.

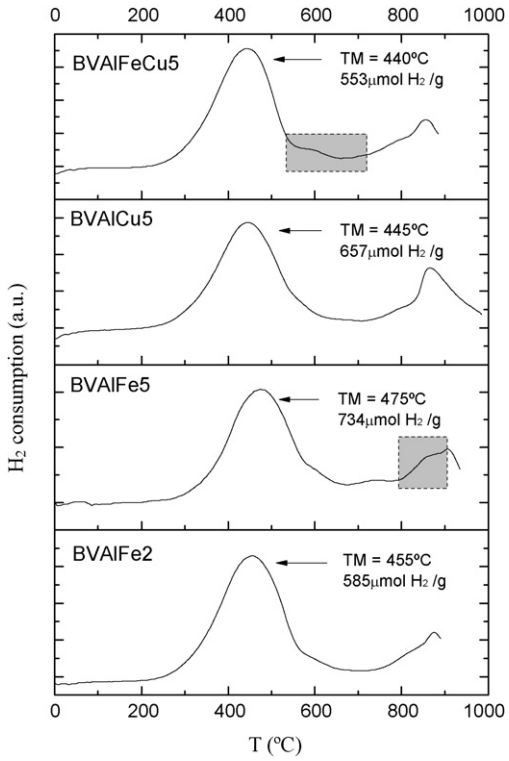

Fig. 4. H_2-TPR diagrams of selected BV-PILCs. TM = temperature of maximum hydrogen consumption.

charge of the polycations and then neither on the charge compensation undergone by the solids upon the pillaring treatment.

The powder X-ray diffraction patterns of the pillared materials derived from BV clay (Fig. 3) show that all of them were expanded up to 1.8–2.0 nm. The solid pillared with pure Al-polycations, BVAl, showed a basal spacing of 1.94 nm. In the case of the Al/Cu-PILCs, it can be noted the basal spacing slightly increasing with AMR, while for Al/Fe-PILCs, when AMR values are low, it is lower than for BVAl solid (i.e., 1.78 nm for AMR 1.0%), whereas for higher values of AMR the basal spacings are similar to those obtained from oriented films. Similar behaviour was observed for Al/Cu-PILCs, but showing slightly higher changes in the basal spacing with AMR. Analysing *fwhm* values (full width at half maximum), it was realized that additions of copper (*fwhm* ~ 1.00–1.10°, 2θ) led to narrower d_{001} peaks than iron additions (*fwhm* ~ 1.15–1.25°, 2θ), behaviour probably related with the higher proportions of Fe than Cu stabilized in the solids.

The H_2-TPR diagrams of some solids of the BV-series are shown in Fig. 4. The solids with AMR = 5.0% were selected, as they have the higher contents in iron and copper, the plot for the solid BVAlFe2 being also included for comparison. In all of them, two broad reduction effects are observed, one from about 250 °C to 580 °C and the other one at around 750–950 °C. The first effect can be ascribed to reduction of iron, which according to Chen and Yan [46] follows a three-step sequence: (1) $Fe_2O_3 \rightarrow Fe_3O_4$; (2) $Fe_3O_4 \rightarrow FeO$; and (3) $FeO \rightarrow Fe$, which appear overlapped in our solids. These signals have been referenced to occur at 465 °C, 545 °C and 673 °C, respectively in Al/Fe-PILCs [47], the first one being claimed to correspond to the reduction α-$Fe_2O_3 \rightarrow Fe_3O_4$ of iron oxide on the surface [28]. In the case of supported copper oxides, several zeolite-like materials have been studied as hosting supports or modified by cationic-exchange with this metal, showing in general H_2-TPR diagrams with two sequential reduction effects in the range 210–260 °C for $Cu^{2+} \rightarrow Cu^{+}$, and at ca. 400–700 °C for $Cu^{+} \rightarrow Cu^{0}$ [48,49]. Very similar temperatures have been observed for the same reduction steps in Cu-ion exchanged or impregnated Ti-PILCs (210–280 °C and 430 °C, respectively), besides to one signal at lower temperature (close to 180 °C) ascribed to CuO aggregates [50], but higher temperatures in the case of Cu impregnated on Al/Ce-PILC (460 °C and 570 °C, respectively) [51]. This shows that for solids where isolated species of Cu can be formed, the temperature of reduction can also vary widely as a function of the support's nature. As long as no signals of hydrogen consumption were observed for our Al/Cu-modified clays below 200 °C, it can be easily inferred that formation of CuO clusters on the clay surface, if any, was negligible in the low AMR values explored, probably because of the very specific mechanism of incorporation of the metal applying the Al/Cu pillaring procedure. Though, as indicated, specific interactions with zeolite-like surfaces induce higher temperatures for the second effect of Cu reduction, in our study no significant H_2 consumption attributable to reduction of Cu species was evidenced above this temperature. It also demonstrates that a significant fraction of the iron present in the starting material is not located in structural sites of the clay, being in consequence more easily reduced at the lower temperatures observed in our first peak. The maximum of this reduction effect appeared at 455 °C for BVAlFe2 solid, at 475 °C for BVAlFe5, at 445 °C for BVAlCu5 and at 440 °C for BVAlFeCu5. As expected, the reduction of Cu^{2+} takes place at lower temperature than that of Fe^{3+}, and the results obtained suggest that, in the three-metallic system, the presence of Cu probably induces Fe to be reduced at lower temperatures. Comparing the two solids of the BVAlFe system, the temperature of reduction increases when the Fe content increases, result opposite to that usually reported when wider ranges of AMR have been employed, where higher iron contents usually led to lower reduction temperatures [52]. This also suggests that a catalytic advantage can be obtained concerning the distribution of

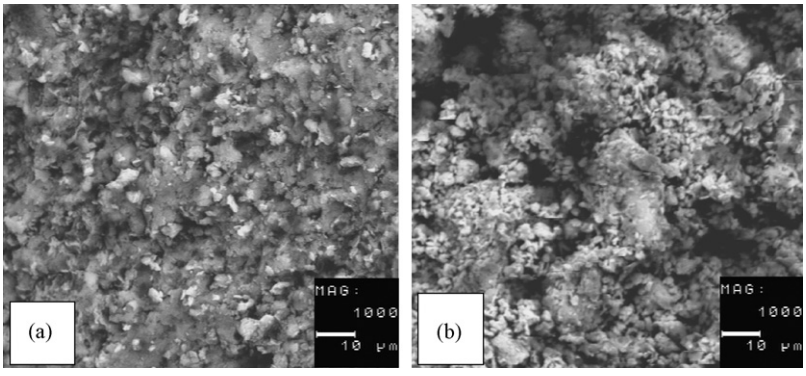

Fig. 5. SEM micrographs for BVAlFe samples with increasing AMR. (a) BVAlFe2; (b) BVAlFe5.

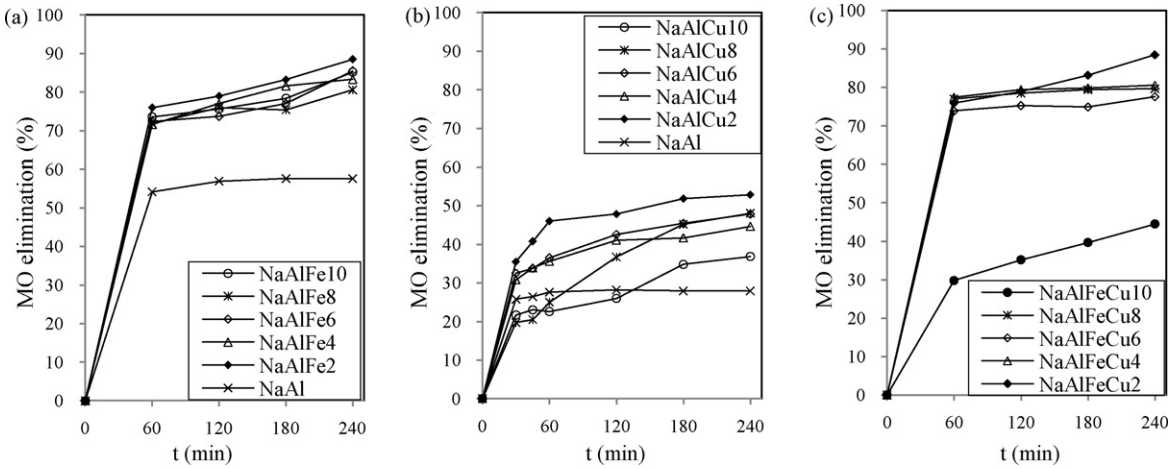

Fig. 6. Catalytic performance of the NaBV-derived PILCs in the elimination of MO at various AMR values: (a) Al/Fe-PILCs (pH = 3.7); (b) Al/Cu-PILCs (pH = 5.5); (c) Al/(Fe–Cu)-PILCs (pH = 4.6). Set up: $[MO]_0$ = 100 mg/L; catalyst loading = 5.0 g/L; $[H_2O_2]$ = 0.15 M; $[H_2O_2]$ addition flow rate = 2.0 mL/h; final stoichiometric ratio $[H_2O_2]/[OIII]_0$ = 0.9; temperature = 18 ± 2.0 °C; pressure = 0.7 atm.

active species by using low AMR values in the modification of clays with Cu or Fe, because the formation of more reducible, less active oxide aggregates (those reducible at lower temperature) of these metals can be almost neglected. In all cases, the peaks of reduction are very symmetric, not allowing their deconvolution to distinguish different effects, which may also be caused by the low content of reducible cations. The effect at temperatures higher than 750 °C has been assigned in other clay mineral, a saponite, to the reduction of structural Fe^{3+}, located in octahedral positions [52].

A comparison between the first signal obtained for the materials modified with AMR = 5.0% shows that besides the shift of the peak maximum, the Al/Fe-modified material exhibits the higher hydrogen consumption, followed by the Al/Cu- and the Al/(Fe–Cu)-modified, respectively. Although it can be due to several reasons, the loading of reducible metals and their relative reducibility play undoubtedly the principal role. Considering the amount of each element fixed by pillaring (Table 1), higher hydrogen consumption is expectable for BVAlFe5 than for BVAlCu5; in fact, it is very feasible that a major fraction of the consumption observed for the last solid does correspond to the iron content in the starting mineral. The lower consumption exhibited by the three-metallic modified system, considering the larger amounts of metals stabilized in it against that achieved for copper in BVAlCu5, could be attributed to lower reducibility of the stabilized species. This behaviour would be properly explained by the presence of three-metallic mixed oxides, perhaps formed in these solids after the pillaring treatment, as proposed recently by Timofeeva et al. [4]. Moreover, when the amount of hydrogen consumed at this reduction step is referred to the net amount of the active metals stabilized in every solid: BVAlFe2 = 1.01, BVAlFe5 = 0.87, BVAlCu5 = 2.73 and BVAlFeCu5 = 0.59 (mmol H_2/mmol stabilized metal(s)), it can be realized that iron and copper together exhibited even lower reducibility (lower hydrogen consumption) in the three-metal system (41% of the hydrogen expected for stoichiometric reduction) than Fe in the binary system Al/Fe (67% and 58% of the hydrogen expected by the corresponding stoichiometric reduction, for BVAlFe2 and BVAlFe5, respectively), which may be due to the formation of less reducible mixed three-metallic oxide phases, as discussed later. However, a comparison between the solids modified with the system Al/Fe (BVAlFe2 and BVAlFe5) let us also to infer that as AMR increases in this short range, the fraction of the active metal retained as more stable, less reducible species also increases, probably in form of mixed bimetallic species which are not reduced in the temperature range of the first broad peak. In the case of the solid BVAlCu5, the total hydrogen consumption is meaningless, as it exceeds the maximum theoretical consumption (1.0 mmol H_2/mmol stabilized Cu) when a complete reduction of the element is supposed. This is related to the undefined amount of extra-structural FeO*x* aggregates coming from the starting material, which remains nearly constant in all the solids and whose hydrogen consumption is inherently included in the calculation, making very difficult to refer it to the Cu content with acceptable accuracy, because of the very low insertion attained for this active metal.

The effects appearing as shoulders close to 600 °C and 850 °C for iron-modified samples (specially those remarked with gray dashed squares in Fig. 4) could be *a priori* attributed to iron oxide aggregates, probably spinel-like phases, formed during the calcination step [2,27,34,53]. In the present samples, it may be considered that Cu^{2+} and Fe^{2+} as divalent cations and Fe^{3+} and Al^{3+} as trivalent ones may participate in the formation of spinel-like phases, and besides Fe_3O_4, $CuFe_2O_4$ probably may be also reducible at this temperature, while $FeAl_2O_4$ may be reduced at higher temperature (see next paragraph).

The reduction effect at higher temperature, as indicated before due to the reduction of octahedral structural iron, shows a shoulder appearing at lower temperature near 850 °C, mainly in the case of BVAlFe5 sample. This shoulder could be reasonably attributed to the reduction of $FeAl_2O_4$, *a priori* the most difficult to reduce of the mixed phases that can be formed by the elements present in the samples and reduced only a few degrees before than structural Fe^{3+} cations of the clay. This effect was also detected and reported by Belver et al. when prepared an Al/Fe-pillared saponite employing AMR values higher than 10% [34]. It is important to note that the intensity of this shoulder clearly increases in the series Al/Fe as AMR raised from 2.0% to 5.0% (BVAlFe2 to BVAlFe5), and it is also observed for the solid BVAlCu5. However, it is also important to point out that these phases were not detected by XRD patterns, which could be expected by their low content and small particle size (in fact, these phases have not been detected by other researchers who assessed the complete compositional range Al–Fe in pillared saponite [52]). Furthermore, as long as we know there are no reports about Fe in spinel-like structures being reduced by H_2 at temperatures so high to be compatible with this shoulder close to 850 °C.

On the other hand, Wan et al. [54], studying iron reduction on Fe-Al_2O_3 catalysts, found that Fe_3O_4 forms FeO instead of direct reduction to elemental Fe, which has been ascribed to a strong Fe–Al_2O_3 interaction; the reduction from FeO to Fe^0 happening at temperatures higher than 570 °C. Therefore, it can be proposed that

the shoulder observed in our TPR study close to 600 °C for the Al/Fe- and the Al/(Fe–Cu)-modified materials, might correspond to the reduction effect of iron oxide aggregates under strong interaction with Al_2O_3, possibly the so-called iron "decorating" the alumina pillars, claimed in some previous studies as the preferential active species generated in Al/Fe-PILCs [2,27,53]. Furthermore, the other shoulder recorded mainly for BVAlFe2 and BVAlFe5 near 850 °C, would be reasonably attributed to true mixed Al/Fe species. It can be rationally supposed that iron in this last kind of species should be H_2-reduced at higher temperatures compared to those displayed by free iron oxides, interlayered iron oxide aggregates or iron oxide decorating alumina pillars, but slightly lower than the metal occupying structural sites of the clay.

Simultaneous TGA/DSC analysis of selected samples (Table 2) showed that the pillaring treatment of the clays leads to lower temperatures for both, dehydration of physisorbed water (T_{M1}) and structural dehydroxilation (T_{M2}), together with a clear increase in the percentage of mass loss in the first thermal event, less evident for the solids of the three-metallic system. Pillaring also enhances the textural properties of the materials in terms of higher specific BET surface area and micropore and total pore volumes, which is a typical feature of pillared clays. The decrease in the central point of the thermal processes can be related to the higher exposition undergone by the interlayer surface of the pillared materials because of the expansion of the layers. This effect is clearly more important for the binary metal systems than for the solid pillared with pure Al-solution (BVAl solid), while small differences are found between the solids of a given series. The mass loss values have a good correlation with the textural properties, and hence, the decrease of both magnitudes for the solids with higher AMR values suggests that the active metals can form external aggregates, which are able to partially block the porosity, mainly the microporosity (Table 2). Comparing the solids in BVAlFe and BVAlCu series to BVAl sample, it is evident that the addition of small amounts of Fe leads to samples with similar textural properties than the solid pillared with pure Al, while the addition of Cu produces a remarkable enhancement of these properties. As already indicated the increase of AMR to the highest values considered in this work provoked a deleterious effect in both series. The behaviour of the three-metallic series is very similar to that of BVAlFe series, as can be expected from the very low amount of Cu fixed. The addition of a second metal (Fe and/or Cu) to the single Al_{13}-intercalation system always led to an increase of the percentage of external surface area with the AMR of the active metals.

SEM micrographs for BVAlFe2 and BVAlFe5 samples show significant changes in the morphology of the particles, although the difference in AMR is low (Fig. 5). As the amount of iron added to the system increases, a greater amount of tiny particles deposited on the clay surface are seen, which may correspond to external oxide aggregates. This behaviour was also observed for the solids of the other two metal systems investigated, Al/Cu- and Al/(Fe–Cu)-PILCs (micrographs not shown for brevity). In opposite trend to chemical analyses, the Fe/Al ratio obtained for these samples by EDX analysis decreased when increasing AMR (0.69 for BVAlFe2 and 0.61 for BVAlFe5), suggesting that a higher percentage of the Fe incorporated to the solid is in the form of intercalated species, which is in agreement with TPR and XRD results.

3.2. Effect of AMR on the catalytic activity of the mixed pillared clays

3.2.1. NaBV-modified materials

Methyl orange has become lately an excellent model toxic molecule alternative to phenol for the catalytic assessment of active solids in Fenton-like reactions, as for instance CWPO [55,56]. This is because its concentration can be easily monitored by visible spectroscopy without demanding further previous treatment of the samples. Although the oxidative pathway of MO by hydroxyl/peroxyl radical reactions must still be studied in greater detail, some previous works have evidenced that there is no incidence of by-products absorbing in the same region of the visible spectrum that might provide some interference [18,57,58]. Hence, the colour decay of MO can be completely ascribed to cleavage of the N=N linkage and used for practical purposes to measure the extent of the catalytic abatement of the azo dye, after which only absorptions of the aromatic residues in by-products remain significant on the UV region. Main by-products of methyl orange obtained through Fenton-AOP reactions have been recently reported by Devi et al. [57].

The catalytic performance of the NaBV solids modified with the three mixed metal systems in the oxidation of methyl orange is compared in Fig. 6. First of all, the clay treated only with Al (NaAl) shows an activity not negligible, reaching a colour elimination close to 50% at pH = 3.7 (Fig. 6a) and almost 30% at pH = 5.5 (Fig. 6b). This catalytic activity can be mainly related to the iron content present in the raw clay mineral (6.95 wt.% Fe_2O_3, dry-basis, Table 1), as it has been referenced elsewhere for the same starting clay also only pillared with alumina [2,59]. The catalytic activity increases for the solids treated with the active metals. As indicated before, the net amount of iron fixed through modification is lower than the iron content present in the starting clay (less than 25%), which clearly indicates that Fe incorporated by pillaring is fairly much more active than that originally present in the clay.

Comparing the activity of the solids from all the series, it is observed that Al/Fe-PILCs are the most efficient, being able to remove close to 80% of MO in only 1 h of reaction. Results from Al/(Fe–Cu)-PILCs are similar, only slightly lower. Although this seems to suggest that addition of Cu does not show any positive effect, the different pH employed for each system may also be considered; since there is a general agreement on pH values 3.0–3.7 [37] as the most favourable range for Fenton reaction to be activated with iron either, under homogeneous or heterogeneous regime, the preservation of the catalytic activity for the Al/(Fe–Cu)-PILCs at pH 4.6 is remarkable. Since the pK_a of MO is 3.46 [60], the anionic form of the toxic molecule predominates at the pH values employed for every one of the catalytic systems, what strongly disregards that simple adsorption of the azo dye might explain the high levels of decolourization observed, as long as the residual CEC of the modified clays should disfavour it seriously. It is well reported that optimal pH for Fenton reactions using Al/Fe-pillared clays is in the neighbourhood of 3.7, where also the rate of the parasite decomposition of peroxide to water and oxygen is minimized [36].

It is also clear that iron catalysts resulted more active than copper modified ones. However, this strongly depends on the net amount of active metal effectively stabilized in each case. It is noteworthy that the concentrations of the active metals in the aqueous effluent after the catalytic tests varied between around 0.5 mg/L and 1.0 mg/L, ruling out a significant homogeneous activity. While these concentrations correspond to leaching values below 3% of the Fe content in the catalysts, they correspond to even more than 50% of leaching in the case of Cu. This can be due to lower stability of Cu in the environment of reaction, but it must be considered that these results are affected by the extremely low amounts of this metal both, fixed in the catalysts and consequently also leached to the effluents during the catalytic tests. Besides, it must be underlined that concentrations of Fe leached from the materials only modified with Al (NaAl and BVAl), were 0.6 mg/L and 0.8 mg/L, respectively, indicating that most of the leaching recorded for the materials treated with active metals came from the starting clays, and the Fe and Cu attached in the materials remained almost completely stable after the catalytic test. This last

assertion can be also derived from the high reusability displayed by the catalysts, as discussed later.

The effect of the AMR value on the catalytic performance in all mixed metallic systems is very interesting. *A priori*, it could be expected that higher proportions of active metals in the final solids would lead to more active catalysts. However, in the series NaAl/Fe-PILCs, all the Fe-containing solids have final catalytic activities almost constant, the most active being the solid with an AMR value of 2.0%. In the series Al/Cu-PILCs the solid with an AMR of 2.0% is also the most active and the activity decreases with the increase of AMR, in some cases being even lower than that of the solid without active metals (NaAl). In the series of Al/(Fe–Cu)-PILCs, the activity remain almost constant for AMR values between 2.0% and 8.0% and markedly decreases for an AMR of 10.0%. This behaviour suggests that the catalytic activity is more influenced by the nature of the metal species formed and the way they are fixed on the clay surface than by the net content of metals inserted into the clay. Hence, despite the fact that a higher AMR value induces a higher statistic probability for the active metal(s) to substitute Al from the structural sites into the Keggin-like polycations, apparently under these conditions there is even greater incidence of extra-structural aggregates of the metal oxides to be formed and deposited on the final catalyst. Hence, for high AMR values, the formation of low-active phases, in particular the oxide aggregates that partially may block the accessibility of the reagents to the more active sites, increases in higher relative proportion than the substitutions of Al in Keggin-like polycations. Thus, a fraction of the active metals is "wasted", being not available for reaction on the solid surface. This observation is in good accord with several works that have claimed that isolated species of the active metal are the main responsible for the high catalytic activity and chemical stability of Al/Fe-pillared clays in the CWPO reaction [3,4,14,19,22,59]. Indeed, Timofeeva et al., from specific studies by ESR and solid state ^{27}Al-NMR spectroscopy, have proposed that the most active species are true mixed pillars exhibiting a Keggin-like formula $(FeAl_{12})^{7+}$ [19,21,22]. Assuming Timofeeva's hypothesis, it seems that the higher formation of mixed pillars is reached in our solids for an AMR of 2.0%; in other words, at this AMR values the efficiency of the incorporated cations is optimal.

It is remarkable that the catalytic performance of these solids runs parallel to the compensation of the cationic capacity (CC); there is a strong correlation between the ability of the polycations to exchange the clay charge and the catalytic performance of the resulting solids for the CWPO reaction. In other words, independently of the amount of iron or copper fixed, when the polycations compensated more CEC of the original clay, the final catalytic activity of the solids was higher. This observation is strong evidence indicating a great specificity of the catalytic activity depending on the nature of the species that these cations can form after intercalation.

The chemical stability and reusability of the best catalysts, those with an AMR of 2.0% in all series (NaAlFe2, NaAlCu2 and NaAlFeCu2), was then checked by performing five consecutive catalytic tests (plots not shown). The loss of catalytic performance of the solids by reuse was imperceptible for the binary systems, in which the MO elimination reached around 85 and 45% for NaAlFe2 and NaAlCu2, respectively, after 1 h of reaction. However, for NaAlFeCu2 the MO elimination reached close to 70% at the same time of reaction, then decreasing steadily to 65% in the fifth catalytic run, probably because of a slow leaching of the active metals during the successive runs.

3.2.2. BV-modified materials

Taking into account the results presented in the previous section, assuming that isomorphic substitution of the active metals (Fe and/or Cu) in the Keggin-like polycations may take place and that mixed pillars are the most active catalytic species in the CWPO reaction, it becomes evident that low AMR values are the most interesting to be explored in detail, particularly the range AMR $\leq$ 5.0%, when looking for the best compromise between catalytic activity and chemical stability. Besides, these values have been scarcely investigated in the literature. For this reason, additional samples with these AMR values were prepared, using a purified fraction of the raw clay as starting material (BV clay, Fig. 2). Some results for the characterization of the obtained solids are given in Tables 1 and 2, and their catalytic behaviour is shown in Fig. 7. In this AMR range, the MO elimination rises with the content of iron and/or copper. Again, the Al/Fe system is confirmed as the most active in the elimination of the toxic molecule reaching eliminations exceeding 90% at 240 min of reaction, regardless the AMR value. Both copper containing systems achieved MO elimination values close to only 70% at the same time of reaction. AMR strongly affects the time required to reach the maximal performance; while the solid BVAlFe1 eliminates around 40% of MO in 30 min of reaction, the sample BVAlFe5 reaches close to 80% at the same time of reaction.

As said before, elimination of the azo dye by simple adsorption on the solids can be clearly ruled out, what can be seen from Figs. 6 and 7. It is evident that the Al/Cu and the Al/(Fe–Cu) systems exhibit lower performance than that from the Al/Fe system.

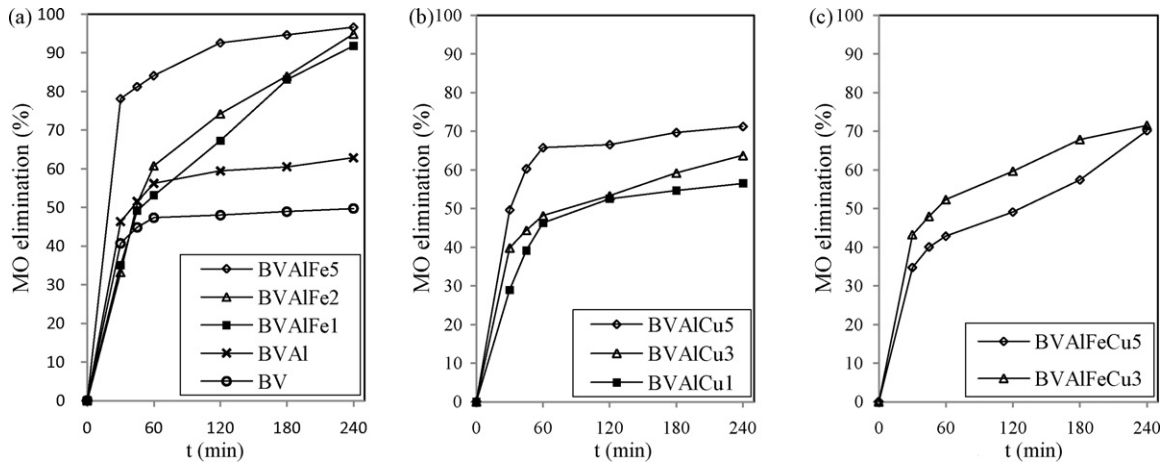

Fig. 7. Catalytic performance of the BV-derived PILCs modified at various AMR values, in the elimination of MO: (a) Al/Fe-PILCs (pH = 3.7); (b) Al/Cu-PILCs (pH = 5.5); (c) Al/(Fe–Cu)-PILCs (pH = 4.6). Set up: $[MO]_0$ = 100 mg/L; catalyst loading = 5.0 g/L; $[H_2O_2]$ = 0.15 M; $[H_2O_2]$ addition flow rate = 2.0 mL/h; final stoichiometric ratio $[H_2O_2]/[OIII]_0$ = 0.9; temperature = 18 ± 2.0 °C; pressure = 0.7 atm.

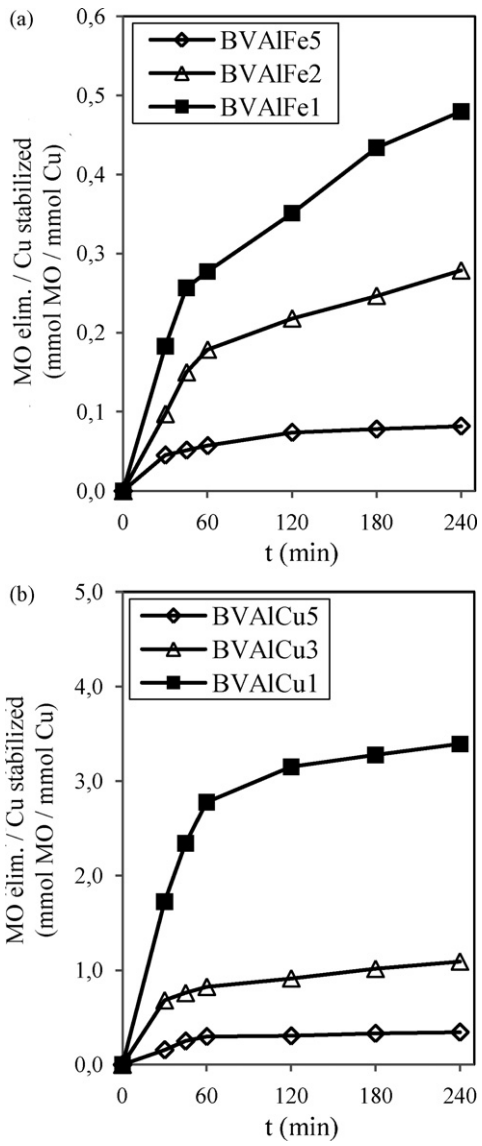

Fig. 8. Catalytic performance of BV-derived materials, referred to the net amount of active metal stabilized in every case. (a) Al/Fe-PILCs; (b) Al/Cu-PILCs.

At this respect, Timofeeva et al. [4] have recently found that higher involvement of Cu in Al/(Fe–Cu)-PILCs (Al/(Fe + Cu) = 10/1) leads to higher catalytic efficiency of the obtained materials in the CWPO reaction of phenol via a lower induction period. However, these authors also found that this catalytic enhancement conduced to lower stability of Fe to leaching, significant decreasing in the specific surface area of the final materials and lower amounts of iron effectively incorporated to the clay, the last parameter being the controller of the rate for full oxidation. Hence, in the AMR range studied in the BV-series (≤5.0%), not induction period for Al/Fe- neither Al/Cu-PILCs was observed, probably because these materials performed a faster reaction rate in the first hour of the tests. It is also worth noting that these authors used materials with AMR of 9.1%, clearly higher than the range explored by us, in which the amount of extra-framework species deposited may significantly block microporosity of the materials being the responsible for the observed induction period in the Al/Fe-system. It may also be underlined that such an induction period was not observed by other researchers working with the same procedure of preparation for Al/Cu-PILCs, while it has been so far reported when copper catalyses the CWPO reaction under homogeneous conditions, due to formation in solution of non-reactive intermediates [61].

If the catalytic activity is referred to the net amount of the active metals stabilized in the binary mixed systems, the catalytic performance per active site significantly decreases as the AMR value increases (Fig. 8). For high AMR values, high formation of external aggregates that strongly worsen the critical physicochemical features like textural properties and charge compensation efficiency may take place. Thus, the best results per active site are obtained for an AMR of 1.0%, for which most of the iron and copper fixed may form very active phases.

4. Conclusions

Al/Fe-, Al/Cu- and Al/(Fe–Cu)-pillared clays were prepared from a Colombian bentonite. The effect of the loading of low amounts of the active metals (Fe and/or Cu) related to Al in the intercalating solutions (AMR ≤ 10%), in the physicochemical and catalytic (aqueous CWPO elimination of methyl orange) properties was investigated. The insertion of low amounts of active metals rose almost linearly with AMR for both binary mixed systems. In the three-metallic system, the stabilization of Cu varied randomly with AMR, while the stabilization of Fe was almost not affected by the presence of Cu. A competition between both active metals for octahedral sites into the framework of Al_{13} polycations is proposed for the three mixed metal systems studied, also explaining why the stabilization of iron is around 15 times higher than that of copper in the binary systems. The compensation of the CEC of the clay by the polycations only depended of AMR for the Al/Fe-system. The basal spacing of the intercalated solids reasonably matched to the size of the different cations, what allowed us to propose that even Cu^{2+} may substitute small amounts of Al^{3+} in the Keggin-like polycations. H_2-TPR curves showed several effects, suggesting the existence for low AMR values in Al/Fe-system, of Fe "decorating" alumina pillars and true mixed pillars. When AMR was higher than 5%, the textural properties worsened, probably by formation of aggregates that blocked the porosity, provoking a decrease of the catalytic activity. AMR > 2% did no longer enhance the catalytic activity, mainly in the Al/Cu-system. This seems to be related to the ability of the polycations to compensate the CEC of the starting clay and to stabilize higher fractions of the active metal(s) as isolated species, not worsening the textural properties. The lower catalytic activity of the Al/Cu-PILCs is due to the very low amounts of Cu stabilized by the pillaring procedure, as their activity referred to the net amount of the active metal stabilized is even higher than for Al/Fe-PILCs.

Acknowledgements

L.A. Galeano acknowledges to *Vicerrectoría de Investigaciones y Postgrados VIPRI-Universidad de Nariño* for the financial support. The authors gratefully thanks also to MEC-FEDER funds (MAT2007-66439-C02).

References

[1] J.H. Ramirez, M. Lampinen, M.A. Vicente, C.A. Costa, L.M. Madeira, Ind. Eng. Chem. Res. 47 (2008) 284–294.
[2] J. Carriazo, E. Guélou, J. Barrault, J.-M. Tatibouët, R. Molina, S. Moreno, Water Res. 39 (2005) 3891–3899.
[3] M.N. Timofeeva, S.Ts. Khankhasaeva, Y.A. Chesalov, S.V. Tsybulya, V.N. Panchenko, E.Ts. Dashinamzhilova, Appl. Catal. B-Environ. 88 (2009) 127–134.
[4] M.N. Timofeeva, S.Ts. Khankhasaeva, E.P. Talsi, V.N. Panchenko, A.V. Golovin, E.Ts. Dashinamzhilova, S.V. Tsybulya, Appl. Catal. B-Environ. 90 (2009) 618–627.
[5] Y. Segura, R. Molina, F. Martínez, J.A. Melero, Ultrason. Sonochem. 16 (2009) 417–424.
[6] A. Rodríguez, G. Ovejero, J.L. Sotelo, M. Mestanza, J. García, Ind. Eng. Chem. Res. 49 (2010) 498–505.
[7] J.A. Botas, J.A. Melero, F. Martínez, M.I. Pariente, Catal. Today 149 (2010) 334–340.

[8] A.L. Barros, T.M. Pizzolato, E. Carissimi, I.A.H. Schneider, Miner. Eng. 19 (2006) 87–90.
[9] R. Andreozzi, V. Caprio, A. Insola, R. Marotta, Catal. Today 53 (1999) 51–59.
[10] G. Centi, S. Perathoner, T. Torre, M.G. Verduna, Catal. Today 55 (2000) 61–69.
[11] M. Pera-Titus, V. García-Molina, M.A. Baños, J. Giménez, S. Esplugas, Appl. Catal. B-Environ. 47 (2003) 219–256.
[12] Y.-P. Chen, S.-Y. Liu, H.-Q. Yu, H. Yin, Q.-R. Li, Chemosphere 72 (2008) 532–536.
[13] J. Barrault, M. Abdellaoui, C. Bouchoule, A. Majesté, J.-M. Tatibouët, A. Louloudi, N. Papayannakos, N.H. Gangas, Appl. Catal. B-Environ. 27 (2000) L225–L230.
[14] E. Guélou, J. Barrault, J. Fournier, J.-M. Tatibouët, Appl. Catal. B-Environ. 44 (2003) 1–8.
[15] A. Rey, M. Faraldos, J.A. Casas, J.A. Zazo, A. Bahamonde, J.J. Rodríguez, Appl. Catal. B-Environ. 86 (2009) 69–77.
[16] P. Bautista, A.F. Mohedano, N. Menéndez, J.A. Casas, J.J. Rodríguez, Catal. Today 151 (2010) 148–152.
[17] K.C. Gupta, A.K. Sutar, Polym. Adv. Technol. 19 (2008) 186–200.
[18] J.H. Ramírez, C.A. Costa, L.M. Madeira, G. Mata, M.A. Vicente, M.L. Rojas-Cervantes, A.J. López-Peinado, R.M. Martín-Aranda, Appl. Catal. B-Environ. 71 (2007) 44–56.
[19] M.N. Timofeeva, M.S. Mel'gunov, O.A. Kholdeeva, M.E. Malyshev, A.N. Shmakov, V.B. Fenelonov, Appl. Catal. B-Environ. 75 (2007) 290–297.
[20] A. Quintanilla, J.A. Casas, J.J. Rodríguez, Appl. Catal. B-Environ. 93 (2010) 339–345.
[21] M.N. Timofeeva, M.E. Malyshev, V.N. Panchenko, A.N. Shmakov, A.G. Potapov, M.S. Mel'gunov, Appl. Catal. B-Environ. 95 (2010) 110–119.
[22] M.N. Timofeeva, S.Ts. Khankhasaeva, S.V. Badmaeva, A.L. Chuvilin, E.B. Burgina, A.B. Ayupov, V.N. Panchenko, A.V. Kulikova, Appl. Catal. B-Environ. 59 (2005) 243–248.
[23] L.A. Galeano, S. Moreno, Rev. Col. Quim. 31 (2002) 57–69.
[24] S. Caudo, C. Genovese, S. Perathoner, G. Centi, Micropor. Mesopor. Mater. 107 (2008) 46–57.
[25] J.H. Ramírez, M.A. Vicente, L.M. Madeira, Appl. Catal. B 98 (2010) 10–26.
[26] W.Y. Lee, B.J. Tatarchuk, Hyperfine Interact. 41 (1988) 661–664.
[27] W.Y. Lee, R.H. Raythatha, B.J. Tatarchuk, J. Catal. 115 (1989) 159–179.
[28] F. Bergaya, N. Hassoun, J. Barrault, L. Gatineau, Clay Miner. 28 (1993) 109–122.
[29] T. Bakas, A. Moukarika, V. Papaefthymiou, A. Ladavos, Clay Clay Miner. 42 (1994) 634–642.
[30] I. Pálinkó, K. Lázár, I. Kiricsi, J. Mol. Struct. 410–411 (1997) 547–550.
[31] I. Pálinkó, A. Molnár, J.B. Nagy, J.-C. Bertrand, K. Lázár, J. Valyon, I. Kiricsi, J. Chem. Soc. Faraday Trans. 93 (1997) 1591–1599.
[32] W. O'Neil Parker Jr., R. Millini, I. Kiricsi, Inorg. Chem. 36 (1997) 571–575.
[33] T. Mandalia, M. Crespin, D. Messad, F. Bergaya, J. Chem. Soc. Chem. Commun. 19 (1998) 2111–2112.
[34] C. Belver, M.A. Vicente, A. Martínez-Arias, M. Fernández-García, Appl. Catal. B-Environ. 50 (2004) 227–234.
[35] S.A. Ong, E. Toorisaka, M. Hirata, T. Hano, Sep. Purif. Technol. 42 (2005) 297–302.
[36] J. Barrault, J.-M. Tatibouët, N. Papayannakos, C.R. Acad. Sci. II C 3 (2000) 777–783.
[37] J.-M. Tatibouët, E. Guélou, J. Fournier, Top. Catal. 33 (2005) 225–232.
[38] A.C.D. Newman, G. Brown, in: A.C.D. Newman (Ed.), Chemistry of Clays and Clay Minerals, Mineralogical Society Monograph No. 6, Mineralogical Society, 1987.
[39] L. Chmielarz, P. Kústrowski, M. Zbroja, B. Gil-Knap, J. Datka, R. Dziembaj, Appl. Catal. B-Environ. 53 (2004) 47–61.
[40] R. Ben Achma, A. Ghorbel, S. Sayadi, A. Dafinov, F. Medina, J. Phys. Chem. Solids 69 (2008) 1116–1120.
[41] J.Y. Bottero, J.M. Cases, F. Fiessinger, J.E. Poirier, J. Phys. Chem. 84 (1980) 2933–2939.
[42] J.Y. Bottero, D. Tchoubar, J.M. Cases, F. Fiessinger, J. Phys. Chem. 86 (1982) 3667–3673.
[43] J. Thorez, Practical Identification of Clay Minerals: A Handbook for Teachers and Students in Clay Mineralogy, Institute of Mineralogy, Liege State University, Belgium, 1976.
[44] N.R. Sanabria, M.A. Centeno, R. Molina, S. Moreno, Appl. Catal. A 356 (2009) 243–249.
[45] R.D. Shannon, Acta Crystallogr. A 32 (1976) 751–767.
[46] K. Chen, Q. Yan, Appl. Catal. A 158 (1997) 215–223.
[47] N.R. Sanabria, R. Molina, S. Moreno, Catal. Lett. 130 (2009) 664–671.
[48] R. Kefirov, A. Penkova, K. Hadjiivanov, S. Dzwigaj, M. Che, Micropor. Mesopor. Mater. 116 (2008) 180–187.
[49] M. Richter, M.J.G. Fait, R. Eckelt, E. Schreier, M. Schneider, M.-M. Pohl, R. Fricke, Appl. Catal. B-Environ. 73 (2007) 269–281.
[50] J.L. Valverde, A. de Lucas, P. Sánchez, F. Dorado, A. Romero, Appl. Catal. B-Environ. 43 (2003) 43–56.
[51] Q. Lin, J. Hao, J. Li, Z. Ma, W. Lin, Catal. Today 126 (2007) 351–358.
[52] C. Belver, M.A. Bañares-Muñoz, M.A. Vicente, Appl. Catal. B-Environ. 50 (2004) 101–112.
[53] A. Gil, L.M. Gandía, M.A. Vicente, Catal. Rev. Sci. Eng. 42 (2000) 145–212.
[54] H.-J. Wan, B.-S. Wu, C.-H. Zhang, H.-W. Xiang, Y.-W. Li, B.-F. Xu, F. Yi, Catal. Commun. 8 (2007) 1538–1545.
[55] N. Pugazhenthiran, S. Ramkumar, P. Sathish Kumar, S. Anandan, Micropor. Mesopor. Mater. 131 (2010) 170–176.
[56] L. Zhang, F. Lv, W. Zhang, R. Li, H. Zhong, Y. Zhao, Y. Zhang, X. Wang, J. Hazard. Mater. 171 (2009) 294–300.
[57] L.G. Devi, S.G. Kumar, K.M. Reddy, C. Munikrishnappa, J. Hazard. Mater. 164 (2009) 459–467.
[58] J. Fernández, J. Kiwi, C. Lizama, J. Freer, J. Baeza, H.D. Mansilla, J. Photochem. Photobiol. A 151 (2002) 213–219.
[59] J.G. Carriazo, R. Molina, S. Moreno, Appl. Catal. A 334 (2008) 168–172.
[60] D.R. Lide (Ed.), CRC Handbook of Chemistry and Physics, 85th ed., 2004, pp. 8–19.
[61] S. Caudo, G. Centi, C. Genovese, S. Perathoner, Top. Catal. 40 (2006) 207–219.